Front. Optoelectron. 2016, 9(3): 420–427
DOI 10.1007/s12200-016-0581-8

REVIEW ARTICLE

Femtosecond laser processing of microcavity lasers

Xuepeng ZHAN, Huailiang XU (✉), Hongbo SUN (✉)

State Key Laboratory on Integrated Optoelectronics, College of Electronic Science and Engineering, Jilin University, Changchun 130012, China

© Higher Education Press and Springer-Verlag Berlin Heidelberg 2016

Abstract In this paper, we reviewed the fabrications of functional microcavity lasers in soft materials such as polymer and protein by femtosecond laser processing. High-quality (Q) microdisks with a laser dye (Rhodamine B, RhB) acting as gain medium were fabricated that produced whispering-gallery-mode (WGM) lasing output. We also obtained unidirectional lasing output with a low lasing threshold in a deformed spiral microcavity at room temperature. Photonic-molecule (PM) microlasers were prepared to investigate the interaction and coupling effects of different cavities, and it was found that the distance between the two disks plays an important role in the lasing behaviors. Single-mode lasing was realized from a stacked PM microlaser through Vernier effect. Furthermore we adopted the biocompatible materials, RhB-doped proteins as a host material and fabricated a three-dimensional (3D) WGM microlaser, which operated well both in air and aqueous environment. The sensing of the protein microlasers to Na_2SO_4 concentration was investigated. Our results of fabricating high-Q microlasers with different materials reveal the potential applications of femtosecond laser processing in the areas of integrated optoelectronic and ultrahigh sensitive bio-sensing devices.

Keywords femtosecond laser processing, microcavity lasers, polymer, protein

1 Introduction

Optical microcavities with small mode volume and high quality (Q) factors have been considered as the basic building blocks of integrated optoelectronic devices, and may have board applications in optical communications, photonic circuits and optical sensors [1–9]. Microcavity lasers based on whispering-gallery-mode (WGM) typically refer to microdisks, microrings, microcylinders and microspheres cavity [10–18], and generally possess some unique lasing features including ultrasmall mode volume and ultrahigh Q factors. Light can be efficiently confined within such WGM microcavities via the total internal reflection of photons at the surface of rotational symmetric cavities, which enhances the interaction of light and matters and improves the lasing performances.

Lots of efforts have been devoted to the tremendous progress in the development of microlaser processing technologies such as photolithography, proton beam writing and reactive ion etching [19–21]. Recently, femtosecond laser processing technique has attracted much attention because of its intrinsic three-dimensional (3D) prototyping capability with ultrahigh spatial resolution [22,23]. Meanwhile the unique features of ultrashort pulse duration of femtosecond laser with high peak power reduce the heat diffusion from the interaction area to surrounding zones in material processing, making the femtosecond laser processing an ideal tool for fabrications of both soft and hard materials such as polymer, protein, glass and crystal [24–29]. Thus a variety of devices including micro-optics, micro-fluidics, micro-electronics and micro-sensing [30–33] have been fabricated in optical transparent materials by femtosecond laser processing [34].

In this paper, we give an overview of our latest progress in the fabrication of high-Q microlasers in soft materials of polymer and protein by the femtosecond laser processing. We begin with a brief description of the homebuilt femtosecond laser processing system, which is followed by presenting several examples for fabricating dye-doped polymer and protein microlasers, whose lasing performances is at room temperature. Subsequently, one example showing the applications of the protein microlasers in environmental sensing is introduced. Lastly, a summary and a future outlook are given.

2 Femtosecond laser processing system of 3D microcavity lasers

A homebuilt femtosecond laser system is shown in Fig. 1

Received December 30, 2015; accepted March 29, 2016

E-mails: huailiang@jlu.edu.cn, hbsun@jlu.edu.cn

[35], in which a Ti:sapphire femtosecond laser system (Spectra Physics 3960-X1BB) with a repetition rate of 80 MHz, a pulse width of 120 fs, and a central wavelength at 800 nm was used as a light source. The laser beam was tightly focused, by a high-numerical-aperture (NA = 1.35) oil-immersion objective lens (100×), on the interface between materials and substrate or inside the materials. To achieve 3D micro/nano fabrications, a piezo stage with 1-nm precision (PI P-622 ZCD) was used to control the sample's vertical movements, and meanwhile a two-galvano-mirror set enabled the beam's horizontal scanning. To control 3D point-by-point scanning, the complicated geometries of micro/nano-structures were designed by softwares including "Visual Basic" and "3D Studio Max", and then converted to computer processing data. The power energy of the laser beam, which is key factor in fabricating process, could be varied continuously by using an attenuator before the oil-immersion objective lens. The host materials were rinsed to remove the unsolidified parts after laser fabrication. As a result the produced 3D microcavity lasers were left on the substrates.

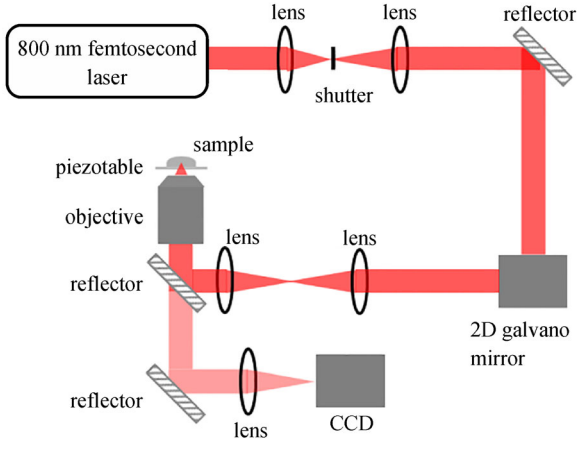

Fig. 1 Schematic diagram of homebuilt femtosecond laser processing system [35]

3 Micro-lasers fabricated by femtosecond laser processing

3.1 Polymer WGM micro-lasers

The fabrications of passive and active microcavities with femtosecond laser processing appeared only at early 2010s [36–38]. In 2011, we fabricated a WGM microdisk laser with the diameter of 20 μm by femtosecond laser direct writing of dye-doped resins [38]. Laser dye of RhB was selected as the gain medium, which was doped into SU-8 negative photoresist with an overall concentration of 1 wt%. As shown in Fig. 2(a), the absorption peaks of RhB-doped SU-8 is centered at around 550 nm, which guarantees the fabrication of the resin materials by two-photon polymerization, but not by the linear absorption. As shown in Figs. 2(b)–2(d), both the existence of the significant threshold (Figs. 2(b) and 2(c)) and the stronger peaks in the spectral range of 610–650 nm (Figs. 2(d) and 2(e)) show the fingerprint of the lasing action at room temperature, when pumped by a frequency doubled Nd:YLF picosecond laser (532 nm, 15 ps, 50 KHz). It was well known that the free spectral range (FSR) is strongly dependent on the dimensions of the microcavity, basing on the WGM fundamental relation of $\Delta\lambda = \lambda^2/(n\pi d)$, where n and d is the effective index and the diameter of the microcavity, respectively. For a fabricated microdisk with a diameter of 30 μm, we measured the FSR, which was 2.635 nm. This agrees well with the theoretically calculated value of ~ 2.602 nm, showing the WGM feature of the fabricated microcavity.

It is well known that Q factor is a typical factor used to evaluate the energy store capability of a cavity, with the equation that $Q^{-1} = Q_{abs}^{-1} + Q_{scat}^{-1} + Q_{cav}^{-1}$, where the

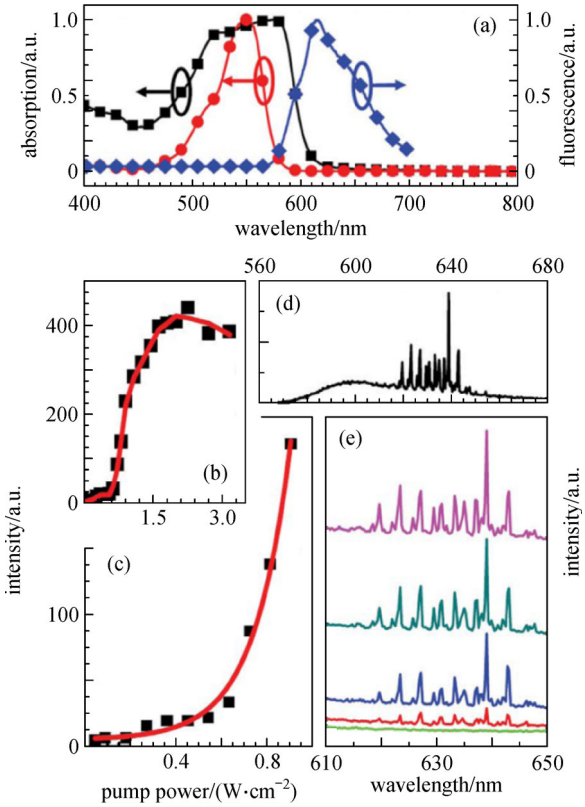

Fig. 2 (a) Absorption spectra of RhB (circle), RhB-doped SU-8 (square) and photoluminescence (PL) spectrum of the mixed resin (diamond); (b) light output versus pumping laser intensity; (c) zoomed-in light output versus pumping laser intensity; (d) emission spectrum in the spectral range of 560–680 nm; (e) emission spectra of microdisk laser at different pumping intensities [38]

inverse of Q_{abs}^{-1}, Q_{scat}^{-1} and Q_{cav}^{-1} correspond to the absorption loss, scattering loss and cavity finesse, respectively [39]. Scattering loss caused by the surface roughness and shape deformation is a key factor in determining the Q value of the microdisk laser. According to $Q = \lambda/\delta\lambda$, where λ is the resonance wavelength and $\delta\lambda$ is the full width at half maximum (FWHM), the Q value of the microcavity is estimated to be $\sim 1.6 \times 10^3$, which is not satisfying. However, the Q factor of the active microcavity may be underestimated when compared with that of a passive one, which normally gives a Q factor at the level 10^6 and even greater [40].

3.2 Unidirectional lasing emission from polymer micro-lasers

Since the isotropic lasing emission of WGM microrelasers with rotational symmetry can result in unavoidable low collection efficiency by lens coupling [41], polymer microlasers providing unidirectional emissions have been recently developed, for example, by the photolithographic method [42]. Recently, we have demonstrated unidirectional emissions from a spiral-shaped polymer microdisk by femtosecond laser processing via two-photon polymerization [43]. In this case, the boundary of the disk could be defined in polar coordinates (r, φ) as $r_{(\varphi)} = r_0\{1 + \varepsilon\varphi/(2\pi)\}$, with ε being the deformation parameter and r_0 the radius at $\varphi = 0$. A meaningful notch part will be created as the radius $r_{(\varphi)}$ jumps back to r_0 at $\varphi = 2\pi$. A typical sample with a diameter of ~30.1 μm and a notch size of 1.6 μm is designed to examine the directional emission property of the spiral-shaped microcavity laser. The thickness of the microdisk is 2 μm.

As shown in the inset of Fig. 3(a), the emission intensity distribution pattern of the spiral cavity is plotted in a polar coordinate and it can be found that the lasing intensity from 0° is much stronger than those measured from other angles, where 0° refers to the direction facing the notch section. It can be seen that the spiral shaped microcavity laser exhibited a good unidirectional lasing emission property with a far field divergence of about 40°. Meanwhile, the peak position of lasing modes emitted from the spiral shaped microcavity shifts with the collection angles, and that the measured lasing thresholds are slightly varied with different angles. This might be due to the chromatic dispersion when light hits the boundary with different incident angle and escapes from the cavity via tunneling. The unidirectional emission is verified (see Fig. 3(b)) by a 2D finite difference time domain (FDTD) numerical simulation, in which clockwise propagating high-Q whispering-gallery like modes might couple to the counterclockwise modes, giving a unidirectional output. The realization of the creation of unidirectional emission lasers in polymer provides an important step toward fabricating functional integrated organic optoelectronic devices by femtosecond laser processing.

3.3 Photonic-molecule polymer microlasers

To investigate the cavity-cavity interactions, photonic-molecule (PM) lasers are good candidates [44,45]. Thus, we fabricated polymer dye-doped PM microcavities by femtosecond laser processing in order to reveal the coupling effects of microcavities [35]. Figure 4 shows the scanning electron microscope (SEM) images of four different planar PM microcavity lasers. The two cavities have the same diameters and thinknesses which are 20 and 2 μm, respectively. The edge distances between the two microdisks are 0.79 μm (Fig. 4(a)), −0.21 μm (Fig. 4(b)), −1.25 μm (Fig. 4(c)) and −2.23 μm (Fig. 4(d)), respectively. By using a frequency doubled Nd:YLF picosecond laser (532 nm, 15 ps, 50 KHz) as the excited source, the lasing spectrum in the range of 615–650 nm are obtained for all the PM microcavity lasers at room temperature. The irregular and multiple modes are observed, which is ascribed to the mode coupling between the two disks, leading to the enhancing or suppressing of the modes through Vernier effect due to the slight structural

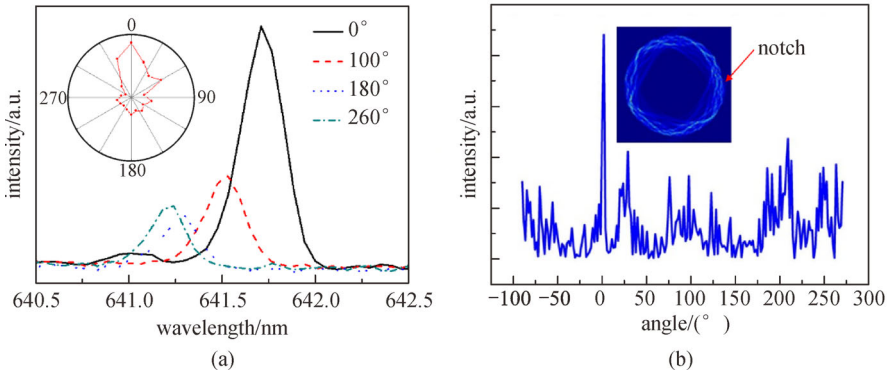

Fig. 3 (a) Room temperature emission spectra of the spiral-shaped disk microlaser. Inset: lasing intensity distribution measured with the signal emitted from different angles; (b) FDTD simulation results of spectral mode structure with the intensity distribution of the mode at 631.65 nm (inset) [43]

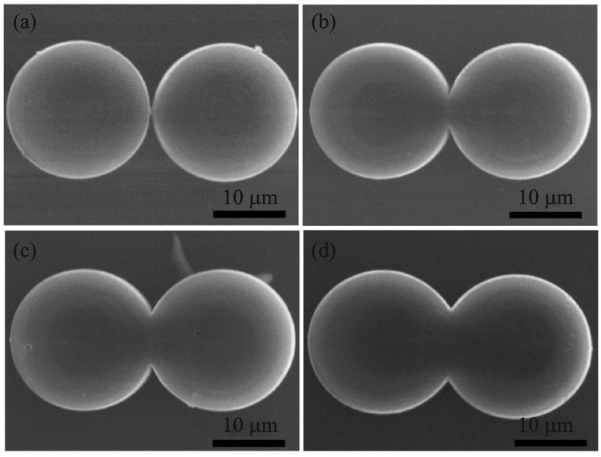

Fig. 4 SEM pictures of planar PM microlasers [35]

difference between the two disks. It is shown that when the overlapping between the two cavities becomes large (see Fig. 4(d)), the intersection of the two disks may destroy the WGM microcavity property. With destroying the circular symmetry of the microcavity in Fig. 4(d), it is found that single mode lasing can be obtained although the threshold energy to achieve lasing becomes much larger in this case.

To further show the single mode lasing from PM lasers, we fabricated a 3D stacked polymer PM dye-doped microcavity lasers [46]. The 3D PM polymer microlaser composes of two identical microdisks stacked with edge alignment, Figs. 5(a)–5(c) show the coupling principle of the two stacked microdisks by Vernier effect. As the excited energy is distributed at the disk periphery and the couple effect happens at the overlapping edge, the intensity of the modes that resonate in both disks could be enhanced largely, while others would be strongly suppressed, providing the possibility to achieve a single-mode lasing output.

Under the optical pump by a frequency doubled Nd:YLF picosecond laser (532 nm, 15 ps, 50 KHz), the spectra of a 3D PM microlaser obtained with different power densities were obtained at room temperature, as shown in Fig. 5(d). It can be seen that the single mode lasing at ~ 642 nm is achieved with a low lasing threshold of 13 W/cm^2. To further reveal the underlying mechanism, the spectrum of another PM microlaser with the diameters of 36 and 60 μm was shown in Fig. 5(e). The intensities of the peaks at 639.1 and 645.3 nm were stronger than others, which indicated that with the mode coupling and competition, these two modes were on resonance simultaneously for both microdisks. According to the WGM relation mentioned above, the FSR_{12} was about 6.2 nm which was five times of FSR_1 obtained from disk diameter of 60 μm, and three times of FSR_2 obtained from the disk diameter of 36 μm. That is, $FSR_{12} = 5*FSR_1 = 3*FSR_2$. This result agrees well with the Vernier effect theory, and further confirm that the coupling of the disks via Vernier effect is the main reason for generating single mode lasing.

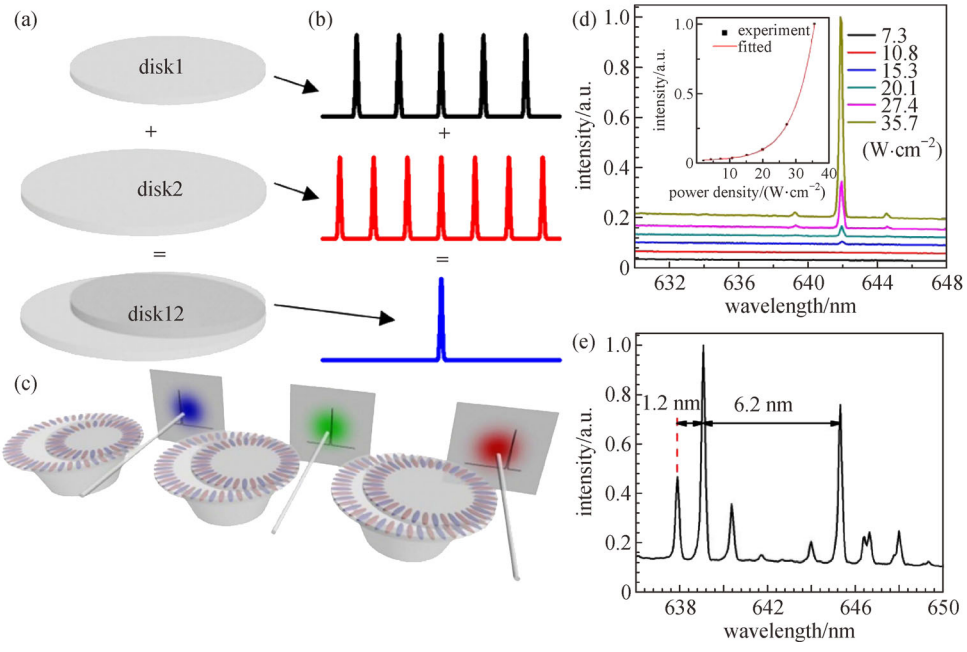

Fig. 5 (a) Schematic diagram of 3D PM microcavity lasers; (b) principle of single-mode lasing via Vernier effect; (c) three lasers are shown by simply changing a small smout of size, temperature, etc. The lasing wavelength can be modulated in a wide range; (d) emission spectrum of 3D PM lasers at different pumping intensities with diameters of 18 and 30 μm. Inset: light output versus the pumping intensity; (e) spectrum with more modes is shown, indicating the Vernier effect [46]

3.4 Protein WGM microlasers

To show the ability of femtosecond laser processing for fabricating different soft materials, we used proteins as the host material to produce 3D WGM microlasers [47]. The promising biocompatible and functionality designable biomacromolecule material, protein (BSA) was photo-cross-linked with the help of self-photosensitization and probable RhB photosensitization without any specific photosensitizers added. In the femtosecond laser processing, the high-viscosity BSA/RhB aqueous ink was well sealed in a small polydimethylsiloxane (PDMS) based chamber to avoid evaporation. After being rinsed in water, the produced protein-based 3D WGM microlasers were left on the substrate.

Under optical pumping of a 532 nm Nd:YLF laser (15 ps, 50 KHz), a laser dye (RhB) doped protein WGM microlaser with the diameter of 30 μm exhibits good lasing action in air without annealing processing. The lasing threshold was ~ 0.57 μW/μm^2 and the FWHM of the lasing line was ~ 0.26 nm at ~ 624.1 nm, which gave rise to the calculated Q factor of ~ 2400 at room temperature. The protein-based WGM microlasers also exhibit valuable steady operation performances in aqueous environments. However, it was found that it was harder to achieve lasing in aqueous environment than in air, we thus fabricated a protein-based 3D WGM active microlaser with the diameter of 60 μm, which gave rise to a Q factors of around ~ 2000 to ~ 3000 in pure water. It should be pointed out that as the equilibrium swelling effect, the diameter of the microcavity in pure water would become a little larger than that in air and the refractive index of the protein hydrogels would decrease slightly. Since the equilibrium-swollen state of protein hydrogels inherently and sensitively responds to the changes of ionic concentration in water, we examined the potential application of the protein-based 3D WGM microlasers in sensing ionic concentration in water, and stimulus-responsive adjust-

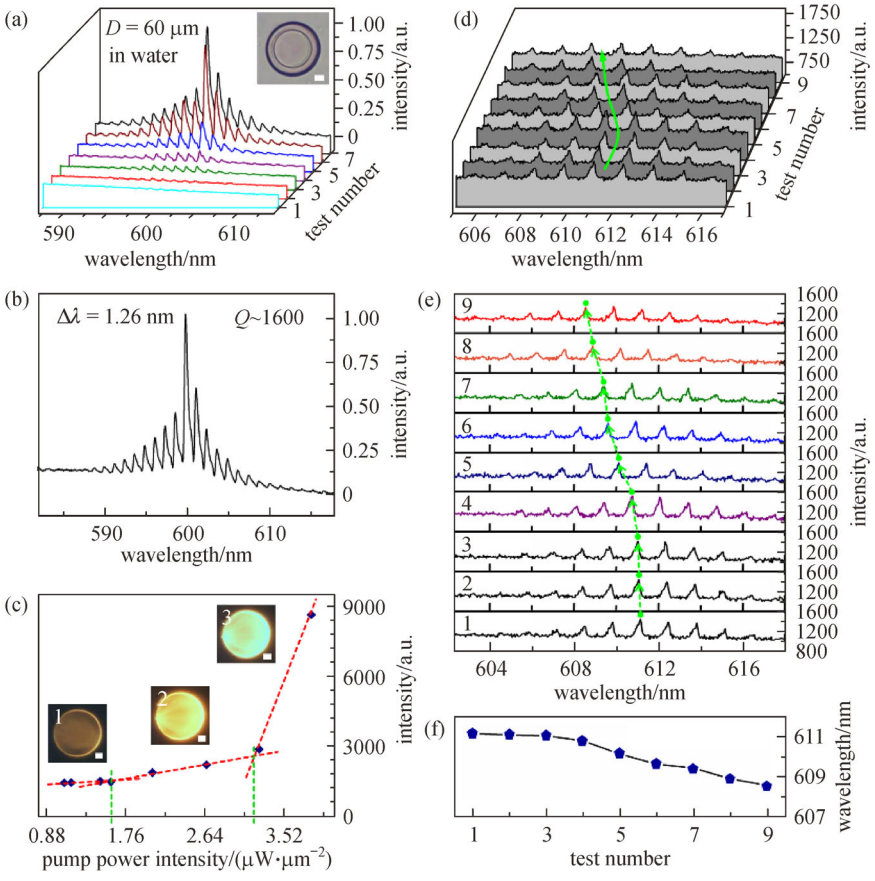

Fig. 6 (a) PL spectra from a 60-μm-diameter protein-based 3D WGM microlaser in pure water. Inset: optical microscopic image; (b) lasing spectrum of test number 7 at room temperature; (c) peak values of PL spectra from the protein-based 3D WGM microlaser versus different pumping intensities. Insets: optical microscopic fluorescent images of samples; (d) 3D-waterfall arranged lasing spectra from the protein-based 3D WGM microlaser in aqueous solutions with increasing Na_2SO_4 concentrations with pumping intensity of ~ 2.0 μW/μm^2; (e) 2D stacked lasing spectra in (d); (f) wavelength blueshift of a particular peak in lasing spectra along with Na_2SO_4 concentration increasing [47]

ment of lasing actions in aqueous environments is investigated by merely changing Na_2SO_4 concentration of aqueous solution.

By gradually increasing the concentration with a step of 8.33×10^{-4} mol/L, the central lasing peak of the protein-based microlaser express a linear blue-shift from ~ 611 to ~ 608.5 nm, as shown in Figs. 6(d)–6(f). That is, the lasing spectrum is responsively blue shifted 2.59 nm when the concentration of the Na_2SO_4 changed (from 0 to 5 mmol/L) by a step of ~ 0.4 nm per 0.83 mmol/L. This reflects that the diameter of microlaser becomes smaller and the effective refractive index increases slightly by hydrogel shrinkage and water extrusion out. It should be noted that the FSR of the coupled disks will be also affected by both the diameter and the effective refractive index of the host materials, and it is found that FSR stays at ~ 1.31 during the test processing with FWHM keeping around 0.2 nm and Q factor remaining at ~ 2000 to ~ 3000. Thus the stimulus-responsive "smart" adjusting with other main performance parameters remained fairly stable in the protein-based 3D WGM microlaser opens new opportunities for biologic and medical applications such as optical biosensing, diagnosis, tunable "smart" biophotonics.

4 Summary and outlook

In summary, we have introduced a homebuilt femtosecond laser processing system and showed our results of fabricating dye-doped microlasers with this homemade system in soft materials including polymer and protein. The oscillations have been achieved in a circular disk and a spiral-shaped disk that produces unidirectional lasing output with a low lasing threshold. Single-mode lasing have also been realized in the stacked PM microlaser by Vernier effect. The cavity-cavity interaction between the two disks in the PM-type microlasers has also been investigated systematically. In addition, we have presented a specific case of the produced protein microlasers operating well both in air and in aqueous solution at room temperature, but showing sensitive response to the Na_2SO_4 concentration. Our demonstrations of fabricating high-Q microlasers by the femtosecond laser processing technique will benefit the potential applications of microlasers in functional integrated optoelectronic and ultrahigh sensitive bio-sensing systems.

References

1. Vahala K J. Optical microcavities. Nature, 2003, 424(6950): 839–846
2. Wiersig J, Gies C, Jahnke F, Aßmann M, Berstermann T, Bayer M, Kistner C, Reitzenstein S, Schneider C, Höfling S, Forchel A, Kruse C, Kalden J, Hommel D. Direct observation of correlations between individual photon emission events of a microcavity laser. Nature, 2009, 460(7252): 245–249
3. Harayama T, Shinohara S. Two-dimensional microcavity lasers. Laser & Photonics Reviews, 2011, 5(2): 247–271
4. He L, Özdemir Ş K, Yang L. Whispering gallery microcavity lasers. Laser & Photonics Reviews, 2013, 7(1): 60–82
5. Ilchenko V S, Matsko A B. Optical resonators with whispering-gallery modes-part II: applications. IEEE Journal of Selected Topics in Quantum Electronics, 2006, 12(1): 15–32
6. Kosma K, Zito G, Schuster K, Pissadakis S. Whispering gallery mode microsphere resonator integrated inside a microstructured optical fiber. Optics Letters, 2013, 38(8): 1301–1303
7. Dai D, Bauters J, Bowers J E. Passive technologies for future large-scale photonic integrated circuits on silicon: polarization handling, light non-reciprocity and loss reduction. Light: Science & Applications, 2012,1(3): e1-1–e1-12
8. Kim K H, Bahl G, Lee W, Liu J, Tomes M, Fan X, Carmon T. Cavity optomechanics on a microfluidic resonator with water and viscous liquids. Light: Science & Applications, 2013, 2(11):e110-1–e110-5
9. Lai Y, Lan Y, Lu T. Strong light–matter interaction in ZnO microcavities. Light: Science & Applications, 2013, 2(6): e76-1–e76-7
10. Grossmann T, Hauser M, Beck T, Gohn-Kreuz C, Karl M, Kalt H, Vannahme C, Mappes T. High-Q conical polymeric microcavities. Applied Physics Letters, 2010, 96(1): 013303
11. Ta V D, Chen R, Sun H D. Self-assembled flexible microlasers. Advanced Materials, 2012, 24(10): OP60–OP64
12. Chen R, Ta V D, Sun H D. Single mode lasing from hybrid hemispherical microresonators. Scientific Reports, 2012, 2: 244
13. Wu Y, Leung P T. Lasing threshold for whispering-gallery-mode microsphere lasers. Physical Review A, 1999, 60(1): 630–633
14. Fang H, Ding R, Lu S, Yang Y, Chen Q, Feng J, Huang Y, Sun H. Whispering-gallery mode lasing from patterned molecular single-crystalline microcavity array. Laser & Photonics Reviews, 2013, 7 (2): 281–288
15. Lu S Y, Fang H H, Feng J, Xia H, Zhang T Q, Chen Q D, Sun H B. Highly stable on-chip embedded organic whispering gallery mode lasers. Journal of Lightwave Technology, 2014, 32(13): 2415–2419
16. Kitur J K, Podolskiy V A, Noginov M A. Stimulated emission of surface plasmon polaritons in a microcylinder cavity. Physical Review Letters, 2011, 106(18): 183903
17. Min B, Ostby E, Sorger V, Ulin-Avila E, Yang L, Zhang X, Vahala K. High-Q surface-plasmon-polariton whispering-gallery microcavity. Nature, 2009, 457(7228): 455–458
18. Jiang X, Zou C, Wang L, Gong Q, Xiao Y. Whispering-gallery microcavities with unidirectional laser emission. Laser & Photonics Reviews, 2016, 10(1): 40–61
19. Armani A M, Srinivasan A, Vahala K J. Soft lithographic fabrication of high Q polymer microcavity arrays. Nano Letters, 2007, 7(6): 1823–1826
20. Huang Y, Lin J, Yang Y, Yao Q, Lv X, Xiao J, Du Y. Unidirectional-emission single mode whispering-gallery-mode microlasers. In: Proceedings of SPIE, Microcavity Lasers and Applications I. 2012, 8236: 1–8
21. Wu X, Li H, Liu L, Xu L. Unidirectional single-frequency lasing from a ring-shaped coupled microcavity laser. Applied Physics Letters, 2008, 93(8): 081105

22. Kawata S, Sun H B, Tanaka T, Takada K. Finer features for functional microdevices. Nature, 2001, 412(6848): 697–698
23. Zhang Y, Chen Q, Xia H, Sun H. Designable 3D nanofabrication by femtosecond laser direct writing. Nano Today, 2010, 5(5): 435–448
24. Liu Z P, Jiang X F, Li Y, Xiao Y F, Wang L, Ren J L, Zhang S J, Yang H, Gong Q. High-*Q* asymmetric polymer microcavities directly fabricated by two-photon polymerization. Applied Physics Letters, 2013, 102(22): 221108
25. Song J, Lin J, Tang J, Liao Y, He F, Wang Z, Qiao L, Sugioka K, Cheng Y. Fabrication of an integrated high-quality-factor (high-*Q*) optofluidic sensor by femtosecond laser micromachining. Optics Express, 2014, 22(12): 14792–14802
26. Lin J, Yu S, Ma Y, Fang W, He F, Qiao L, Tong L, Cheng Y, Xu Z. On-chip three-dimensional high-*Q* microcavities fabricated by femtosecond laser direct writing. Optics Express, 2012, 20(9): 10212–10217
27. Lin J, Xu Y, Fang Z, Wang M, Song J, Wang N, Qiao L, Fang W, Cheng Y.Fabrication of high-Q lithium niobate microresonators using femtosecond laser micromachining. Scientific Reports, 2015, 5: 8072
28. Lin J, Xu Y, Tang J, Wang N, Song J, He F, Fang W, Cheng Y. Fabrication of three-dimensional microdisk resonators in calcium fluoride by femtosecond laser micromachining. Applied Physics A, Materials Science & Processing, 2014, 116(4): 2019–2023
29. Ta V D, Chen R, Sun H. Coupled polymer microfiber lasers for single mode operation and enhanced refractive index sensing. Advanced Optical Materials, 2014, 2(3): 220–225
30. Joshi M P, Pudavar H E, Swiatkiewicz J, Prasad P N, Reianhardt B A. Three-dimensional optical circuitry using two-photon-assisted polymerization. Applied Physics Letters, 1999, 74(2): 170–172
31. Zhang Y, Guo L, Wei S, He Y, Xia H, Chen Q, Sun H, Xiao F. Direct imprinting of microcircuits on grapheme oxides film by femtosecond laser reduction. Nano Today, 2010, 5(1): 15–20
32. Xu B B, Xia H, Niu L G, Zhang Y L, Sun K, Chen Q D, Xu Y, Lv Z Q, Li Z H, Misawa H, Sun H B. Flexible nanowiring of metal on nonplanar substrates by femtosecond-laser-induced electroless plating. Small, 2010, 6(16): 1762–1766
33. Xia H, Wang J, Tian Y, Chen Q D, Du X B, Zhang Y L, He Y, Sun H B. Ferrofluids for fabrication of remotely controllable micro-nanomachines by two-photon polymerization. Advanced Materials, 2010, 22(29): 3204–3207
34. Wang J, He Y, Xia H, Niu L G, Zhang R, Chen Q D, Zhang Y L, Li Y F, Zeng S J, Qin J H, Lin B C, Sun H B. Embellishment of microfluidic devices via femtosecond laser micronanofabrication for chip functionalization. Lab on a Chip, 2010, 10(15): 1993–1996
35. Huang Q, Zhan X, Hou Z, Chen Q, Xu H. Polymer photonic-molecule microlaser fabricated by femtosecond laser direct writing. Optics Communications, 2016, 362: 73–76
36. Grossmann T, Schleede S, Hauser M, Beck T, Thiel M, von Freymann G, Mappes T, Kalt H. Direct laser writing for active and passive high-*Q* polymer microdisks on silicon. Optics Express, 2011, 19(12): 11451–11456
37. Liu Z, Jiang X, Li Y, Xiao Y, Wang L, Ren J, Zhang S, Yang H, Gong Q. High-*Q* asymmetric polymer microcavities directly fabricated by two-photon polymerization. Applied Physics Letters, 2013, 102(22): 221108
38. Ku J F, Chen Q D, Zhang R, Sun H B. Whispering-gallery-mode microdisk lasers produced by femtosecond laser direct writing. Optics Letters, 2011, 36(15): 2871–2873
39. Sasaki F, Kobayashi S, Haraichi S, Fujiwara S, Bando K, Masumoto Y, Hotta S. Microdisk and microring lasers of thiophene–phenylene co-oligomers embedded in Si/SiO_2 substrates. Advanced Materials, 2007, 19(21): 3653–3655
40. Grossmann T, Schleede S, Hauser M, Beck T, Thiel M, von Freymann G, Mappes T, Kalt H. Direct laser writing for active and passive high-*Q* polymer microdisks on silicon. Optics Express, 2011, 19(12): 11451–11456
41. Juodkazis S, Fujiwara K, Takahashi T, Matsuo S, Misawa H. Morphology-dependent resonant laser emission of dye-doped ellipsoidal microcavity. Journal of Applied Physics, 2002, 91(3): 916–921
42. Ben-Messaoud T, Zyss J. Unidirectional laser emission from polymer-based spiral microdisks. Applied Physics Letters, 2005, 86(24): 241110
43. Zhan X P, Ku J F, Xu Y X, Zhang X L, Zhao J, Fang W, Xu H L, Sun H B. Unidirectional lasing from a spiral-shaped microcavity of dye-doped polymers fabricated by femtosecond laser direct writing. IEEE Photonics Technology Letters, 2015, 27(3): 311–314
44. Hara Y, Mukaiyama T, Takeda K, Kuwata-Gonokami M. Photonic molecule lasing. Optics Letters, 2003, 28(24): 2437–2439
45. Grossmann T, Wienhold T, Bog U, Beck T, Friedmann C, Kalt H, Mappes T. Polymeric photonic molecule super-mode lasers on silicon. Light: Science & Applications, 2013, 2(5): e82-1–e82-4
46. Ku J F, Chen Q D, Ma X W, Yang Y D, Huang Y Z, Xu H L, Sun H B. Photonic-molecule single-mode laser. IEEE Photonics Technology Letters, 2015, 27(11): 1157–1160
47. Sun Y, Hou Z, Sun S, Zheng B, Ku J, Dong W, Chen Q, Sun H. Protein-based three-dimensional whispering-gallery-mode microlasers with stimulus-responsiveness. Scientific Reports, 2015, 5: 12852

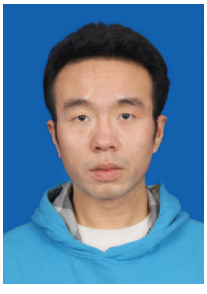

Xuepeng Zhan received his B.S. degree from Jilin University in 2012 and now pursues his Ph.D. at the College of Electronic Science and Engineering of Jilin University. His current research is mainly related to the fabrication of micro/nano-scale structures by femtosecond laser processing.

Huailiang Xu received his Ph.D. degree in physics from Lund University of Sweden in 2004. He then worked as a postdoctoral researcher at Laval University of Canada. In January 2008, he became an assistant professor at The University of Tokyo, Japan. Since September 2009, He has been a full professor at Jilin University, China. His research interests are ultrafast intense laser science, laser fabrication, and atomic and molecular spectroscopy.

Hongbo Sun received his Ph.D. degree in electronics from Jilin University in 1996. He worked as a postdoctoral researcher at University of Tokushima from 1996 to 2000, and then as an assistant professor at Osaka University. In 2005, he was promoted as a full professor in Jilin University. He was awarded the Outstanding Young Scientist Award issued by the minister of MEXT (Japan) in 2006. His research interests are laser nanofabrication and ultrafast spectroscopy.